Scaling of Confinement with Major and Minor Radius in the Tokamak Fusion Test Reactor

L. R. Grisham, S. D. Scott, R. J. Goldston, M. G. Bell, R. Bell, N. L. Bretz, C. E. Bush, B. Grek, G. H. Hammett, K. Hill, F. Jobes, D. Johnson, S. Kaye, D. Mansfield, D. Mueller, H. K. Park, A. Ramsey, J. Schivell, B. Stratton, E. J. Synakowski, G. Taylor, and H. H. Towner

Princeton University Plasma Physics Laboratory, P.O. Box 451, Princeton, New Jersey 08543

(Received 26 December 1990)

Plasma-size scans have been performed in the Tokamak Fusion Test Reactor to investigate the effect of major and minor radius upon energy confinement in high-recycling plasmas heated by neutral-beam injection. The major radius, minor radius, and aspect ratio were varied over a large range (a =0.4–0.9 m, R =2.08–3.2 m, R/a =2.8–8.0). The energy confinement measured with diamagnetic and kinetic diagnostics scales strongly with major radius, and weakly or negatively with minor radius.

PACS numbers: 52.55.Fa

Performance estimates for future tokamak experimental devices and extrapolations to fusion reactor designs rely largely upon empirical scaling relations which describe the energy confinement as a function of global parameters. The largest body of data exists for the L mode [1], the standard confinement regime which obtains for high-recycling auxiliary-heated tokamak plasmas. Regression analyses [2–4] of multiple-tokamak L-mode databases have yielded power-law scaling relations for the variation of total stored energy (W_t) with plasma current (I_p), major radius (R), minor radius (a), and heating power (P_t). The deduced scalings of W_t with size were bounded by $W_t \propto R^{0.85 \rightarrow 1.75}$ and $W_t \propto a^{-0.37 \rightarrow +0.3}$, with the sum of the exponents on R and a remaining in the range 1.3 ± 0.2. These global confinement scaling results suggest that radial heat transport decreases with inverse aspect ratio r/R ($W_t \propto a^2 R^0$ would obtain if heat transport were independent of toroidicity). If verified, a strong favorable dependence of local heat transport coefficients on r/R would help resolve a current paradox in tokamak physics, namely, that local thermal diffusivities are consistently observed to increase with minor radius, both in absolute magnitude and relative to most theoretical predictions. However, the accuracy of the inferred size scaling may be compromised by several factors, including a limited range of aspect ratios studied (R/a =2.4–4), a collinearity between R and a, and uncertainties such as differing diagnostic calibrations and wall conditioning among the tokamaks. A comprehensive evaluation of tokamak energy confinement by the international design team for ITER [4] has identified the geometric scaling of τ_E as a major unresolved issue due to R/a degeneracy in the existing data set. This work breaks the R/a degeneracy in the data set by avoiding collinearity in R and a.

We report two experiments on the Tokamak Fusion Test Reactor (TFTR). The first compares the stored energy in pairs of plasmas with different major radii, but with similar values of other parameters which correlate strongly with global confinement (a, I_p, P_b, n_e, q_c). These studies provide the most unambiguous determination of the R and R/a dependence of energy confinement within the context of L-mode scaling. The second experiment was designed to determine the relative importance of I_p and R/a for the fusion product $\langle nT \rangle \tau_E$ by scanning R/a while adjusting I_p to maintain $I_p R/a$ constant. These data are important since tokamak reactor designers find it valuable to trade I_p against R/a at approximately constant cost and fusion product [5–7], in order to optimize parameters such as bootstrap current fraction and divertor performance.

The TFTR has a carbon toroidal belt limiter on the inner wall and two carbon poloidal ring limiters on the outer wall. The first experiment directly compared the stored energy of pairs of plasmas formed on the inner or outer limiters (see Table I). The toroidal field for all discharges in this paper was adjusted to maintain q_c =3.0–3.2, with the exception of the R/a =3.2/0.4 plasmas which had q_c =2.54. All plasmas were dominated by auxiliary power ($P_b/P_{\mathrm{Oh}} \geq 10$). Gas puffing maintained densities high enough to suppress the (calculated) beam-ion stored energy to (20–33)% of W_t, values typical of the L mode, but low enough to permit good beam penetration, with beam peaking factors $h(0)$ in the range 1.4–3.2. Beam first orbit and shinethrough losses were calculated to be small (total $< 5\%$). Fokker-Planck calculations indicate small ($< 15\%$) power losses due to ripple even for small plasmas on the outer limiter. The plasma density and Z_{eff} in discharges on the outer limiter rose continuously throughout the 250-msec beam pulse, although τ_E was equilibrated within 50–80 msec. The electron-density rise during beam injection was roughly twice as large in outer-limiter plasmas as in inner-limiter ones of the same I_p and P_b, suggesting factor-of-2 differences in limiter recycling. For these plasmas $\beta_p < 1.2$, while the normalized $\beta \equiv \beta_t/(I_p/aB_T)$ was 0.8–1.6, well away from the Troyon limit of 3–4.

The energy content of these plasmas was determined from diamagnetic measurements, and independently by integrating the measured temperature and density profiles over the plasma volume, added to the energy content of unthermalized beam ions as calculated from a numerical solution of the Fokker-Planck equation by the SNAP [8] code, which assumes classical beam deposition, confinement, and thermalization. $T_e(r)$ was measured by 76-

TABLE I. Comparison of stored energy for similar plasmas on the inner and outer limiters. Both the total and electron stored energy show strong R scaling, as indicated by $m_{\rm dia}$ and m_e, the exponents for $W_{\rm dia} \propto R^m$ and for $W_e \propto R^m$. Units are in m for a and R, MA for I_p, MW for P_b, and keV for $T_e(0)$.

a	R	I_p	P_b	n_e	$Z_{\rm eff}$	$T_e(0)$	$m_{\rm dia}$	m_e
0.43–0.40	2.08	0.40	4.5	3.4	1.5	2.2	1.59	2.11
	3.20	0.40	4.4	5.4	3.3	2.0		
0.50	2.15	0.50	6.5	5.6	1.2	1.7	1.72	2.15
	3.10	0.50	6.3	5.1	3.6	2.0		
0.61	2.26	0.63	8.6	4.7	1.4	1.6	1.59	1.85
	2.99	0.63	8.5	5.6	2.4	1.6		

point Thomson scattering, and in some cases by electron-cyclotron-emission (ECE) radiometry and Michelson interferometry as well. $T_i(R)$ was measured by charge-exchange recombination spectroscopy with 10-cm spatial resolution, and $n_e(r)$ by Thomson scattering and by a ten-channel infrared interferometer. Complete $T_i(R)$ profiles were obtained for about $\frac{1}{2}$ of the discharges. For the remainder, where only a portion of the profile was measured, SNAP calculated $T_i(r)$ assuming that the ion thermal diffusivity was equal to a multiple of the electron thermal diffusivity ($\chi_i = c\chi_e$, where c was chosen to reproduce the most central T_i measurement). The deduced values of c ranged from 2 to 4, consistent with our other plasmas and with typical values in large ($a > 0.8$ m) plasmas in the TFTR [9]. The ion density was determined from $n_e(r)$ using $Z_{\rm eff}$ derived from measurements of visible bremsstrahlung emission.

Expressed in power-law form, the observed R scaling for the diamagnetic total stored energy is approximately $W_{\rm dia} \propto R^{1.6-1.7}$ (Table I). The R scaling of the total electron energy content, $W_e \propto R^{1.85-2.15}$ [obtained by integrating the Thomson $T_e(r)$ and $n_e(r)$ profiles], is slightly stronger than that for $W_{\rm dia}$. ECE radiometer T_e profiles were available for both the inner- and outer-limiter 40-cm plasmas, yielding a scaling $W_e \propto R^{2.11}$, virtually identical to that obtained with Thomson scattering. The $Z_{\rm eff}$ is higher in each case for the outer-limiter discharge, which increases the ion-depletion factor and is partially responsible for the difference in scaling of W_e and $W_{\rm dia}$.

For studies of plasma performance scaling at constant I_pR/a, the range of aspect ratio was augmented by the addition of $a = 0.73$ and 0.90 m plasmas on both the inner and outer limiters. Figure 1 shows the dependence of $\langle nT\rangle\tau_E$ upon aspect ratio for $I_pR/a = 3.1$ and 4.3 MA, including data at a variety of beam powers (4–10 MW for $I_pR/a = 3.1$ MA and 8.5–18 MW for $I_pR/a = 4.3$ MA). The $\langle nT\rangle\tau_E$ values were derived from diamagnetic measurements of total stored energy ($\langle nT\rangle\tau_E = \tau_E^{\rm dia} W_{\rm tot}^{\rm dia}$/volume). We find that $\langle nT\rangle\tau_E$ is, at most, a weak function of aspect ratio for I_pR/a fixed, validating tokamak reactor designs which trade off high I_p for large R/a. Comparing the two scans, we see that $\langle nT\rangle\tau_E$ increases roughly as $(I_pR/a)^{2.4\pm0.2}$. There is no observed dependence of $\langle nT\rangle\tau_E$ on beam power, consistent with standard L-mode scaling [1] for which $\tau_E \propto P_b^{-0.5}$.

Power-law regressions of the form $W \propto R^{c1}a^{c2}I_p^{c3}P^{c4}$ were performed for a combined data set including both the paired plasmas and the scans at constant I_pR/a. Within this data set, the aspect ratio varied from 2.8 to 8.0, P_b from 4 to 18 MW, and I_p from 0.4 to 1.5 MA. Only plasmas with $W_{\rm beam}/W_t < 0.3$ were used in the regressions. By the construction of these experiments, there is very little correlation between R and a (correlation coefficient $= -0.15$), but there are strong correlations among P_b, I_p, and a (correlation coefficients ≈ 0.8). As shown in Table II, the regressions on magnetic and kinetic $W_{\rm tot}$ yield similar dependences on I_p and $P_{\rm tot}$. The kinetic data indicate a somewhat stronger scaling on R ($W_{\rm tot} \propto R^{1.77}$ vs $R^{1.51}$), the difference being comparable to the uncertainty in the individual exponents. The magnetic $W_{\rm dia}$ data set can be adequately described by the ITER power-law scaling [4] multiplied by 0.8, while the kinetic data are better described by Goldston scaling [1]. The slight difference between the magnetic and kinetic R scaling arises from systematic differences between the magnetic and kinetic measurements of W_t, which were generally small [kinetic measurements were typically (0–15)% greater than magnetic], except for the 40-cm plasmas on the outer limiter, for which the kinetic measurements exceeded the magnetic by (25–30)%. We con-

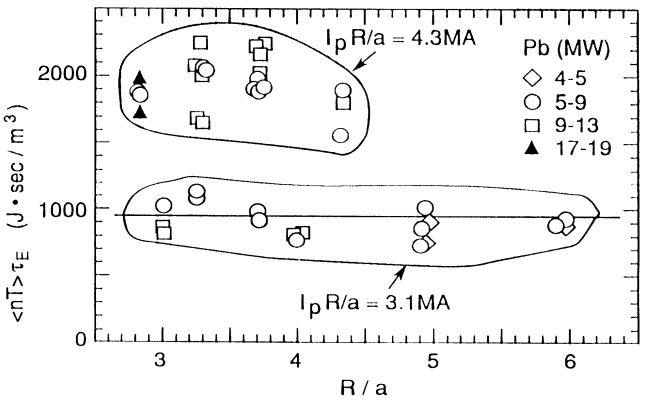

FIG. 1. The fusion performance parameter $\langle nT\rangle\tau$ as a function of R/a for two values of I_pR/a.

TABLE II. Exponents and regression errors from regression analysis of stored energy, where $W \propto R^{c1} I_p^{c2} a^{c3} P^{c4}$. $W_{th} = W_e + W_i$. The estimated standard deviation of the model error is (6.2–7.5)% except for W_e/η, for which it is 12%. Since $q = a^2 B_t / R I_p$ is not varied, the scalings could be multiplied by q^λ for any λ without changing the quality of fit.

	R	I_p	a	P
W_{dia}	1.51	1.16	−0.07	0.44 [a]
W_{kin}	1.77	1.12	−0.24	0.34 [a]
W_{kin}/η	1.99	1.20	−0.51	0.47 [a]
W_{th}	1.53	1.12	−0.25	0.33 [b]
W_e	1.84	1.06	−0.15	0.38 [b]
W_e/η	2.00	1.12	−0.45	0.54 [b]
Error	±0.13	±0.08	±0.12	±0.06

[a] P_{tot}. [b] P_{th}.

sider the kinetic profile measurement of W_t preferable for these plasmas because their low stored energy approaches the accuracy of the diamagnetic measurement, and because all three T_e profile measurements for the 40-cm outer-limiter plasmas yielded the same W_e to within 5%. The accuracy of the T_e measurements is further substantiated by the excellent agreement ($\approx 10\%$) between the measured neutron emission and that calculated from the measured profiles for total d-d reactions (which are strongly dominated by the beam-target contribution). By contrast, the estimated systematic errors on measured $T_i(0)$ of 0.5 keV are a significant fraction of $T_i(0)$ (=1.2–3.2 keV), so the scaling of W_i is less well determined.

Both the kinetic and magnetic W_{tot} show strong R scaling, as do W_{th} and W_e. Within the regression uncertainty, these values for the R scaling are in quite good agreement with the results of the paired plasma comparisons. The I_p scaling is similar for all the regressions. The dependence of W upon minor radius for all these regressions is weak or slightly negative. Note that the total stored energy is scaled against $P_{tot} = P_b + P_{Oh}$, while the thermal scalings use the calculated power delivered to the thermal plasma. The P_{th} scalings of W_{th} and W_e are similar to the scaling found for W_{th} in full-size ($a > 0.9$ m) low-aspect-ratio plasmas on the TFTR [9]. Figure 2 shows plots of W_{dia} and W_e divided by their corresponding deduced scaling relations of Table II, plotted against R/a. The interleaving of the outer- and inner-limiter plasmas, without contradiction of the overall trend, indicates that the different limiter geometries do not seriously bias the data. This is further supported by the observation that two $a = 0.9$ m plasmas at the same I_p and P_b, which were run on the inner and outer limiters with only a slight difference in R/a ($R/a \approx 3$), had almost no difference in stored energy.

The correlation of density with plasma size is weak in the combined data set, e.g., correlation coefficients of −0.1 for n_e and R, and −0.03 for n_e and a, so the inferred size scaling changes little if density is included in

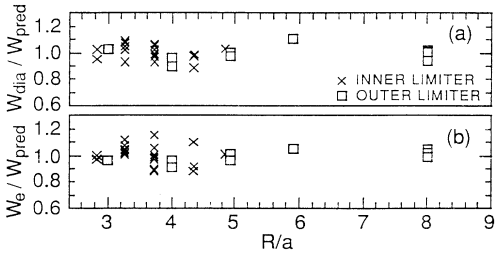

FIG. 2. The measured W_{dia} and W_e divided by their deduced scalings, plotted against aspect ratio.

the regression analysis. For example, we find $W_e \propto I_p^{1.07} R^{1.82} a^{0.07} n_e^{0.3} P_{th}^{0.22}$ and $W_{dia} \propto I_p^{1.16} R^{1.52} a^{-0.13} \times P_{tot}^{0.48} n_e^{-0.1}$, indicating changes of less than 0.02 and 0.22 in the R and a exponents, which are within the combined uncertainties of the regressions compared. Allowing the regressions to include a toroidal field (B_T) or Z_{eff} dependence does not significantly affect the strong R and weak or negative a scaling, although the error bars increase. For instance, the R exponent for W_e becomes 1.79 ± 0.18 if B_T is included, or 2.2 ± 0.3 if Z_{eff} is included instead. The a exponent becomes 0.01 ± 0.42 with B_T included, or -0.28 ± 0.15 with Z_{eff}. In either case the exponent inferred for the added parameter is weak (0.1 ± 0.25 for B_T, and -0.16 ± 0.12 for Z_{eff}).

The observed lack of a positive dependence of confinement on minor radius is contrary to the scaling one would expect for a diffusive heat transport mechanism unless (a) the heat deposition profile $h(r)$ becomes significantly less centrally peaked with increasing minor radius or (b) local heat transport coefficients depend on some quantity correlated with toroidicity (r/R). Systematic variations in $h(r)$ appear unlikely to explain the lack of minor-radius scaling because the average radius of power deposition (normalized to a) varies by less than 35% across the data set. To normalize for differences in heating profile among the various plasmas, one can compute the heating effectiveness parameter [10] η, which represents the ratio of stored energy obtained with a distributed heating profile to that one would expect with a point source at the magnetic axis. As shown in Table II, dividing the stored energy by η has only a small, negative effect on the minor-radius scaling, and a small, positive effect on the power scaling [because the density and therefore $h(r)$ correlate with beam power]. We conclude that the variation of $h(r)$ is not masking a significant positive dependence of confinement on minor radius.

To examine the significance of local toroidicity to heat transport in these plasmas where the ion-electron power exchange is large, we consider an average thermal diffusivity defined as $\chi^{avg} = P_{flux}/(n_e \nabla T_e + n_i \nabla T_i)$, where P_{flux} is the total power flowing through a flux surface, utilizing the measured temperature and density profiles and the calculated heat deposition profile. Figure 3 shows χ^{avg} as a function of local inverse aspect ratio

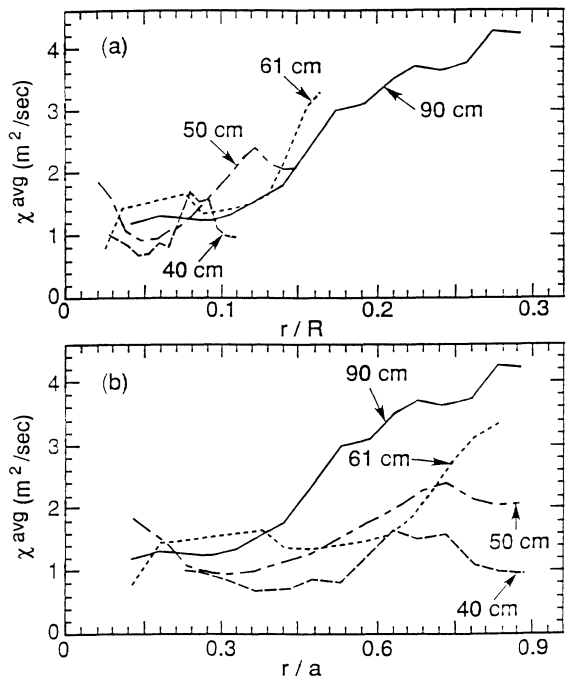

FIG. 3. Comparison of χ^{avg} for various sized plasmas on the outer limiter plotted against r/a and r/R. Plasma conditions were $P_b = 4.3$, 6.0, 6.0, and 6.0 keV; $T_e(0) = 2.0$, 2.1, 1.8, and 2.2 keV; $n_e = 5.4\times10^{19}$, 5.1×10^{19}, 4.9×10^{19}, and 3.3×10^{19} m^{-3}; $I_p = 0.4$, 0.5, 0.63, and 1.04 MA; and $R/a = 8$, 6, 4.9, and 3 for $a = 40$, 50, 61, and 90 cm, respectively. The combination of radiation ($P_{rad}/P_b < 25\%$) and convection dominate the power balance outside $r/a > 0.7$.

(r/R) and of local fractional radius (r/a) for discharges of varying minor radius on the outer limiter described. By the nature of this data set the different plasmas are not identical; nonetheless, the salient feature of Fig. 3 is that local transport appears to be better characterized by r/R than r/a, indicating that high-aspect-ratio plasmas resemble the central cores (at similar local aspect ratio) of larger-minor-radius plasmas with lower global aspect ratio, and suggesting that toroidicity influences local transport. These results suggest that it is the low local aspect ratio of the outer plasma region, rather than the low T_e or high q, which causes χ to rise towards the outside of low-aspect-ratio plasmas.

In conclusion, we find that W_{tot} scales as $R^{1.5-1.7}$ from diamagnetic measurements or $R^{1.7-1.8}$ from profile measurements. The electron stored energy scales as $R^{1.8-2.1}$ from redundant $T_e(r)$ diagnostics. The thermal (ions plus electrons) R scaling ($W_{th} \propto R^{1.5}$) is similar to or somewhat weaker than the W_{tot} scaling, but is less well determined due to larger uncertainties in W_i, and is biased downwards by systematic differences in Z_{eff} between the inner and outer limiters. The confinement scaling with minor radius is weak, and perhaps negative. Plasma fusion performance as measured by $\langle nT\rangle\tau_E$ is relatively insensitive to aspect ratio for a fixed value of I_pR/a, which may allow greater flexibility in tokamak designs. Local heat transport appears to depend in part upon the local inverse aspect ratio, which is consistent with the weak minor-radius scaling of stored energy, and is supportive of a strong role for trapped particle and/or bad curvature effects in turbulent transport.

It is a pleasure to thank Dr. R. Hawryluk, Dr. K. McGuire, Dr. D. Meade, and Dr. D. Post of the Princeton Plasma Physics Laboratory, and Professor R. Conn of the University of California at Los Angeles for their encouragement and interest. This work was supported by U.S. DOE Contract No. DE-AC02-76-CHO-3073.

[1] R. Goldston, Plasma Phys. Controlled Fusion **26**, 87 (1984).
[2] K. S. Riedel and S. M. Kaye, Nucl. Fusion **30**, 731 (1990).
[3] S. Kaye and R. Goldston, Nucl. Fusion **25**, 65 (1985).
[4] P. Yushmanov *et al.*, Nucl. Fusion **30**, 1990 (1990).
[5] W. T. Reiersen, J. A. Schmitt, and D. B. Montgomery, in *Proceedings of the Thirteenth Symposium on Fusion Energy, Knoxville, 2–6 October 1989* (IEEE, New York, 1989).
[6] N. A. Uckan *et al.*, *ITER Physics Design Guidelines: 1989,* ITER Document Series No. 10 (IAEA, Vienna, 1990).
[7] F. Najmadadi *et al.*, University of California at Los Angeles Report No. UCLA-PPG-1323, 1990 (to be published).
[8] H. Towner and R. Goldston, Bull. Am. Phys. Soc. **29**, 1304 (1984).
[9] S. Scott *et al.*, Phys. Fluids B **2**, 1300 (1990).
[10] J. Callen *et al.*, Nucl. Fusion **27**, 1857 (1987).